AN ADAPTIVE FINITE ELEMENT FRAMEWORK FOR FATIGUE CRACK PROPAGATION

Dan Givoli , Ron Zusman
Department of Aerospace Engineering
Technion — Israel Institute of Technology
Haifa 32000, ISRAEL

Keywords: *Finite Element, Fatigue Crack Propagation, Fracture, Adaptive Mesh, Mixed Mode*

Abstract

A new adaptive Finite Element (FE) framework for Fatigue Crack Propagation (FCP) analysis is proposed. This framework combines the simplicity of standard industrial FCP analysis with the generality and accuracy of a full FE analysis and can be implemented by combining standard existing computational tools. In this way it constitutes an attractive alternative to existing approaches. Some novel features are introduced in several of the steps of the proposed scheme in order to make it efficient and at the same time reasonably accurate. A two-dimensional numerical example involving FCP in a thin sheet under plane-stress conditions is presented to demonstrate the scheme's performance. The numerical results are compared to those of laboratory experiments.

1 Introduction

Fatigue Crack Propagation (FCP) analysis has become essential and standard in the design and safety assessment of aircraft structures. In most cases, the analysis performed in industrial applications involves a number of simplifying assumptions and relies mainly on simple analytical or semi-analytical tools and on accumulated experimental data. One assumption that is commonly made in this type of analysis is that the geometry and loading are sufficiently simple so that an *analytical or empirical expression for the Stress Intensity Factor (SIF)* is available. Another frequent assumption is that the given geometry and loading give rise to a *pure-mode* problem, i.e., Mode I or II or III, or at least to a problem dominated by one of these modes. A third assumption is the propagation of the crack being *self-similar*, e.g., in the Mode-I-dominated case it elongates in a straight line perpendicular to the tensile load applied in the far field.

Under such simplifying assumptions it is possible to apply the analytical-empirical methods of classical linear fracture mechanics, described, e.g., in [1]–[3]. Some very useful software products, such as FM [4], are based on these methods and are used constantly in the aerospace industry for damage tolerance analysis. This type of analysis is simple and robust and can be performed even on a personal computer. Its deficiency is that it is limited to cases with simple geometry and load, or, if applied to more complicated cases, it provides only a rough approximation.

On the other end of the spectrum, a detailed two- or three-dimensional Finite Element (FE) simulation is sometimes performed. Due to the complexity of such analysis, it is used today mainly in academic research, or in special and critical cases where high accuracy is needed, like the investigation of a specific failure. The difficulties in this type of analysis are that it usually requires a large computational effort, that it is composed of several stages which are not automatically interconnected, and that it requires a very highly-skilled user. Typical examples for

detailed three-dimensional FCP analysis include [5]–[7]. The general case is that of *mixed-mode* crack behavior [8] and of *non-similar growth*, namely propagation along a path which is not predetermined.

The purpose of the present paper is to propose an adaptive FE framework for FCP analysis which is based on linear elastic theory and *employs standard FE and mesh generation tools*. This framework combines the simplicity of the standard industrial FCP analysis with the generality and accuracy of the full FE analysis. In this way it constitutes an attractive and balanced alternative to the existing approaches. The framework is fully automatic and is constructed in a modular way. Some novel features are introduced within some of its steps in order to obtain an efficient scheme which is at the same time also reasonably accurate. These include a non-standard calculation of the crack opening force, and an approximate implementation of the maximal tangential stress criterion that requires no stress calculation.

2 The FCP-FE Framework

2.1 General Structure of the Framework

The FCP-FE framework employs the following two standard computational tools:

- A mesh generator, also capable of refining the mesh in a specified region.
- An FE stress analysis code.

To these existing tools, a short "driver" code must be added, that iteratively invokes these two tools and performs the simple calculations indicated below.

The framework consists of the following main steps:

1. Mesh generation of the crack-less model.
2. FE analysis of the crack-less model; storing the nodal stresses σ_{ij}^0.
3. Introduction of initial crack in the model.
4. Update of geometrical model.
5. Mesh generation; refining around the crack-tip.
6. FE analysis.
7. Calculation of crack driving force G.
8. Calculation of SIF.
9. Unstable fracture occurs or crack reaches boundary? If yes, stop.
10. Crack arrests? If yes, stop.
11. Calculation of crack propagation rate da/dN.
12. Calculation of crack propagation direction.
13. Final number of cycles reached? If yes, stop.
14. Return to Step 4.

Now some more details are given on each of these steps.

2.2 Step 1: Mesh Generation of the Crack-less Model

In this first step, the initial geometry of the model is read, and an FE mesh is generated according to the user specifications. The crack-less model is needed for later FCP calculations.

2.3 Step 2: FE Analysis of the Crack-less Model

Standard FE stress analysis is performed for the crack-less model. In particular, the averaged stress values at the nodes σ_{ij}^0 are stored for later use. All the other results (deformation, stresses at Gauss points, etc.) of this analysis are discarded.

2.4 Step 3: Introduction of Initial Crack

The initial crack may be introduced either according to the user's specifications or according to some crack initiation criterion. In the former case, the user must specify the location of the

crack root, its initial size and its initial direction. In the latter case, the location and direction are determined by the crack initiation criterion (e.g., according to the location and direction of the maximum principal stress in the crack-less model), and the user only specifies the initial size.

2.5 Step 4: Update of Geometrical Model

The geometrical model consists of the coordinates and connectivity of the entire *boundary* of the elastic body under consideration. After an initial crack is introduced, and also after the crack is elongated in each iteration, the previous coordinates and connectivity must be appropriately modified to accommodate the two newly added crack surfaces.

2.6 Step 5: Mesh Generation and Refinement

The new domain including the crack is meshed. This is done either by generating a totally new mesh, or by locally modifying the previous mesh (depending on the capabilities of the mesh generator at hand). A small region around the crack-tip should be refined. Usually a light refinement is sufficient, since the FCP calculations that follow rely essentially on the crack displacements and not on the stresses (see Step 7 below), and thus *an accurate determination of the stress field around the crack-tip is not needed*. This refinement may be relaxed or even totally avoided if singular quadratic elements are used near the crack-tip, with midside nodes relocated at quarter-distance locations. The use of such elements (or other appropriate singular elements) is recommended; however non-singular (say, standard linear) elements are usable too as long as the mesh is appropriately refined.

2.7 Step 6: FE Analysis

Standard FE analysis is performed. Although the given fatigue loading is cyclic, the FE analysis is static, using a representative loading parameter $\lambda = \lambda_0$ (e.g., unity). Due to the linearity of the elasticity problem, such a representative load is sufficient to scale the entire response of the structure to the cyclic loading (see Step 11 below).

The only results which are needed for later FCP calculations are the displacements at all the nodes along the two crack surfaces (for Step 7) and the principal directions of the stresses at the crack-tip (for Step 12). The other results of this analysis may be retained for display but they are not needed for the FCP analysis.

2.8 Step 7: Calculation of Crack Driving Force

By definition, the crack driving force (also called the energy release rate) is

$$G = -\frac{\partial \Pi_c(a)}{\partial a}\,, \tag{1}$$

where Π_c is the potential energy associated with the crack (or, more precisely, the difference between the potential energy in the body with and without a crack), and a is the crack length. There are several indirect ways to calculate G (e.g., using the J-integral); however, here G is calculated directly by using the finite difference approximation of (1),

$$G(a) = -\frac{\Pi_c(a) - \Pi_c(a-\Delta a)}{\Delta a}\,, \tag{2}$$

where Δa is the crack increment.

A standard formula for G, based on deriving a simplified expression for the difference $\Pi_c(a) - \Pi_c(a-\Delta a)$, is (see, e.g., [2], p. 162, with a slightly different notation):

$$G(a) = \frac{1}{2\Delta a}\int_{a-\Delta a}^{a} \delta u_i^a(s)\sigma_{ij}^{a-\Delta a}(s)n_j(s)\,ds\,. \tag{3}$$

Here s is the coordinate along the crack, and $u_i^a(s)$ is the displacement in the i direction, at location s along the crack, computed for the model with crack-length a. Similarly, $\sigma_{ij}^{a-\Delta a}(s)$ is the ij-stress component at location s, computed for the model with crack-length $a-\Delta a$. The quantity δu_i is the distance (in the i direction) between the two crack surfaces due to the deformation (positive if the crack "opens"), and n_j is the j component of the unit vector $\boldsymbol{n}$ normal to the crack surface. The

difficulty with the formula (3) is that it involves the *singular* stresses $\sigma_{ij}^{a-\Delta a}$ which are unbounded at the crack-tip $s = a - \Delta a$. To avoid this difficulty, (3) is replaced by the following formula for $\Pi_c(a)$:

$$\Pi_c(a) = -\frac{1}{2}\int_0^a \delta u_i^a(s)\sigma_{ij}^0(s)n_j(s)\,ds\,. \qquad (4)$$

This formula is used, in a recursive manner, together with (2) to compute $G(a)$. The integral appearing in (4) is completely *regular*, since σ_{ij}^0 is the stress for the crack-less model and is thus bounded everywhere. It can be shown that (2) and (4) are indeed equivalent to (3).

2.9 Step 8: Calculation of Stress Intensity Factor

The effective mixed-mode SIF K is calculated from the crack driving force G using a well-known relation. Under plane stress conditions this relation is

$$K = \sqrt{EG}\,, \qquad (5)$$

where E is the material Young modulus.

2.10 Step 9: Checking Unstable Fracture and Crack Reaching the Boundary

The SIF K is compared to the material fracture toughness K_c to determine whether unstable fracture occurs with the current geometry and loading. It should be noted that K is the effective Mode-I SIF (i.e., K_I) and similarly $K_c = K_{Ic}$, in accordance with the notion that even in a mixed-mode situation the crack is propagated in an effective Mode-I manner [1].

In addition, if the crack reaches or crosses any boundary of the geometrical model then the analysis is stopped. On the continuous level the SIF always increases beyond the critical value before the crack reaches the boundary; however this is not always the case on the discrete level, especially if the SIF experiences a rapid growth. Also, the analyzer may wish to follow the probable crack path beyond the onset of fracture, and thus would set K_c to an artificially high value.

2.11 Step 10: Checking Crack Arrest

Two criteria are used to determine crack arrest. First, crack propagation stops if the driving force G becomes non-positive. Second, crack closure occurs when the maximal principal stress at the crack-tip is non-positive, namely when the normal stresses around the crack-tip are all compressive.

2.12 Step 11: Calculation of Crack Propagation Rate

Calculation of the current FCP rate is performed using the empirical Paris law:

$$\frac{da}{dN} = C(\Delta K)^m\,. \qquad (6)$$

Here N is the number of cycles, and C and m are material constants. The quantity ΔK is defined as $\Delta K = K_{\max} - K_{\min}$, where $K_{\min}$ and $K_{\max}$ are the two extreme values of K corresponding to the two extreme values of the cyclic loading parameter, $\lambda_{\min}$ and $\lambda_{\max}$. Owing to the linearity of the elasticity problem and the fact that a loading parameter λ_0 has been used in the FE analysis (Step 6 above), it is easy to see that

$$\Delta K = \frac{\lambda_{\max} - \lambda_{\min}}{\lambda_0}\,K\,. \qquad (7)$$

The Paris law (6) may be used in two forms. If the number of loading cycles ΔN in each iteration is fixed, then the current crack increment is calculated via

$$\Delta a = \Delta N\, C(\Delta K)^m\,. \qquad (8)$$

On the other hand, if the crack increment Δa is set to be fixed, then the number of loading cycles needed for this increment is

$$\Delta N = \Delta a / \left[C(\Delta K)^m\right]\,. \qquad (9)$$

The latter mode of calculation should usually be preferred, since in this mode the computational parameters are easier to control.

2.13 Step 12: Calculation of Crack Propagation Direction

Three criteria for determining the current crack propagation direction [8] are implemented:

- *Maximum tangential stress criterion.* The crack propagates in the direction perpendicular to the principal direction corresponding to the maximal tensile stress at the crack-tip. In two dimensions the principal direction θ_P, relative to the global system of coordinates (x,y), is found by $\tan 2\theta_P = 2\sigma_{xy}/(\sigma_{xx}-\sigma_{yy})$; thus only this *ratio* of stresses at the crack-tip need to be found and not the values σ_{ij} separately, which are theoretically infinite. Numerical experiments show that even if the FE analysis does not treat the singularity at the crack-tip properly, the stress ratio obtained is sufficiently accurate to determine the approximate crack direction.

- *Maximum tangential stress criterion, asymptotic calculation.* In order to avoid altogether the need to calculate stresses around the crack-tip, one may proceed as follows. According to the asymptotic formulae for the stress field around the crack-tip [1, 2] the normal opening displacement δu_N is proportional to $K_I\sqrt{r}$ whereas the tangential sliding displacement δu_T is proportional to $K_{II}\sqrt{r}$, *with the same constant of proportionality* that depends on the material properties. Here r is the radial distance from the crack-tip. Thus, $\delta u_T/\delta u_N = K_{II}/K_I$ for $r \to 0$. In practice, the ratio K_{II}/K_I is calculated based on the displacement at the node adjacent to the crack-tip. In turn, the desired maximum principal direction is immediately determined by this ratio [1, 8]:

$$\tan\frac{\theta_m}{2} = \frac{1}{4}\frac{K_I}{K_{II}} \pm \frac{1}{4}\sqrt{\left(\frac{K_I}{K_{II}}\right)^2 + 8}\,. \quad (10)$$

  Note that two approximations are involved in this calculation: (a) the use of the asymptotic expressions for the near stress field; and (b) the calculation of the displacement ratio at a finite distance from the crack-tip. On the other hand, the advantage of this criterion is that it is based on displacements only.

- *Crack-tip displacement criterion.* The crack propagates in the direction perpendicular to the limiting direction of the displacement vector $\delta\boldsymbol{u}(s)$ (see Step 7 above) as s approaches the crack-tip. In practice, the displacement vector at the node adjacent to the crack-tip is used to this end.

For each of these three criteria, a certain amount of random deviation in the crack propagation direction may be added if desired.

2.14 Steps 13 and 14: Closing the Loop

At the end of each iteration, the current accumulated number of cycles N is compared to a given bound; if N is larger than this bound then the process is stopped. Otherwise, one proceeds to the next iteration.

3 Numerical Examples

The computational framework is applied to a problem which is also investigated experimentally in the laboratory. All the specimens used here are thin rectangular sheets, with thickness 3.28mm, made of Aluminum 6061-T6. A "crack gage" is attached to each specimen, which electronically measures, during the entire duration of the experiment, the projected length of the crack in the initial crack direction. In addition, an attached millimetric grid is used to read the same projected length visually. Tensile loads are applied to the specimens by using an MTS loading rig.

First a calibration experiment is performed in order to determine the Paris constants C and m (see (6)) for the material at hand. This experiment was done under pure Mode I conditions, and yielded the values $m = 4.02$ and $C = 6.2\cdot 10^{-14}$ in MPa and m units. These material constants, as well as the known mechanical

properties of aluminum, i.e., Young's modulus $E = 7.3 \cdot 10^4$ MPa and Poisson's ratio $\nu = 0.3$, are used in all the simulations that follow.

Now the specimen described in Fig. 1 is considered. An initial crack of size 6mm is introduced in a sheet of dimensions 10cm×8cm, that contains an off-centered hole. The specimen is loaded in tension in two small regions near its lower and upper ends, as illustrated in the figure. It should be remarked that the loading on the upper end of the sheet has little effect on the stress field and deformation in the regions of interest, and has been applied in the experiment for technical reasons related to the loading surfaces of the MTS machine. The overall tensile force is oscillating between a very small value, which may be regarded as zero, and a maximum value of 1500Kgf. The initial loading frequency was initially set to 10 cyc/sec, but as the crack started to propagate more rapidly the frequency was gradually reduced down to a value of 1 cyc/sec.

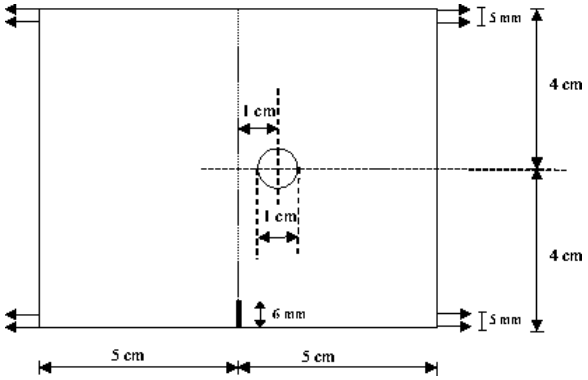

Fig. 1 The FCP specimen

As expected, in the laboratory experiment the crack propagated self-similarly up to a certain point, and then bent and approached the hole. The propagation rate increased gradually during the growth until the crack reached the hole boundary, but no unstable fracture was observed. The experiment was repeated twice. Thus four crack paths have been measured, namely the paths at both sides of the two sheets. Due to the relative large thickness of the sheet and the fact that the crack is slanted in a 45 degree position, the paths obtained on both sides were not identical.

This experiment is now compared to the results of the computation. In the latter, linear triangular finite elements are used throughout. In the analysis described here, a constant crack increment of $\Delta a = 5$mm per iteration is given, and ΔN is computed according to (9). Also, the maximum tangential stress criterion (with no random deviation) is used to determine the crack direction. Two discretized models have been used: a full-length model, and a "reduced model," which is truncated on the right, left and upper part, so that the dimensions of the sheet are 5cm×8cm. Whereas numerical experiments show that the results of the two models are quite similar, the latter requires much less computational effort.

Fig. 2 describes the reduced sheet model with the initial crack, and the corresponding finite element mesh. Fig. 3 shows the deformed model

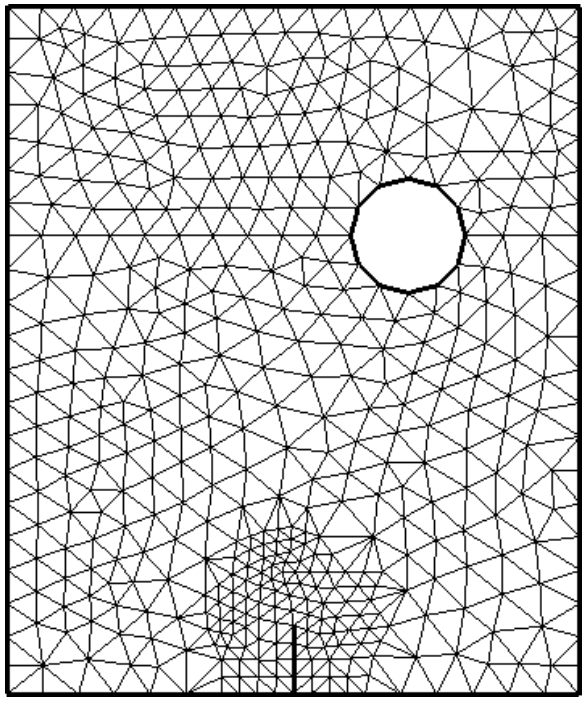

Fig. 2 The computational FCP model: initial crack and mesh

with the final crack path and mesh, as obtained after 8 iterations. In Fig. 4, five crack paths are compared: the four experimental paths and the computational path. Taking into account the large

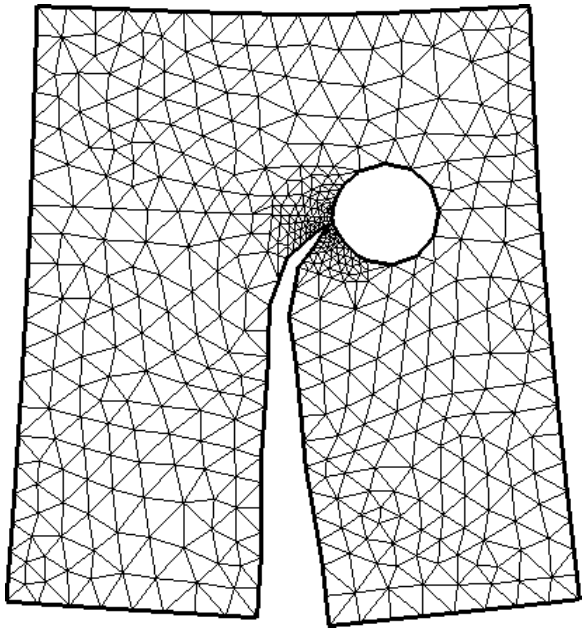

Fig. 3 The computational FCP model: final crack path and mesh in deformed configuration

distribution exhibited in the experimental results, the agreement between computation and experiment is quite satisfactory.

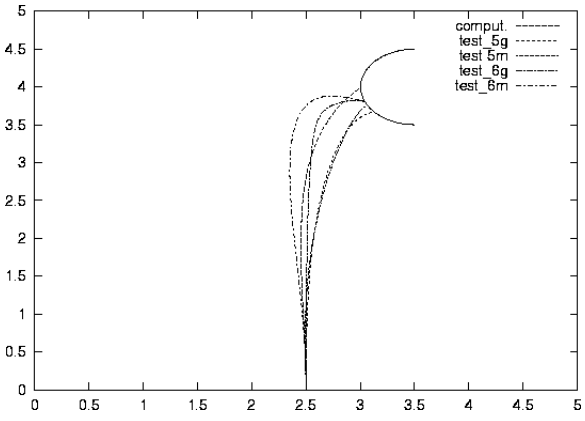

Fig. 4 Experimental and computational Crack paths

The experimental and computational FCP rates were also compared and were found to be in good agreement in average. Again the experimental propagation rates obtained in the two experiments deviated significantly. One effect which causes such a deviation is the sensitivity of the results to the initial amount of cycles needed to initiate the crack growth, which depends on the surface quality and exact geometry of the initial crack.

Acknowledgments

This work is partly supported by the Fund for the Promotion of Research at the Technion. The first author would like to thank Prof. A. Bercovich, A. Putzi Grunwald and R. Yaffe for their help and advice with the laboratory experiments.

References

[1] D. Broek, *The Practical Use of Fracture Mechanics*, Kluwer, London, 1989.

[2] M.F. Kanninen and C.H. Popelar, *Advanced Fracture Mechanics*, Oxford University Press, Oxford, 1985.

[3] S. Suresh, *Fatigue of materials*, Cambridge University Press, Cambridge, 1998.

[4] D. Broek, *Software for Practical Fracture Mechanics and Damage Tolerance Analysis* (Manual), Fracture Research Inc., Galena, Ohio, 1998.

[5] C.-S. Chen, P. Wawrzynek and A.R. Ingraffea, "Methodology for Fatigue Crack Growth and Residual Strength Prediction with Applications to Aircraft Fuselages," *Comput. Mech.*, **19**, 527–532, 1997.

[6] A.S. Gullerud, R.H. Dodds, R.W. Hampton and D.S. Dawicke, "3-D Finite Element Modeling of Ductile Crack Growth in Thin Aluminum Materials," in Fatigue and Fracture Mechanics, Vol. 30, K.L. Jerina and P.C. Paris, Eds., ASTM, 1998.

[7] M. Ortiz, "Computational Micromechanics," *Computational Mechanics*, **18**, 321–338, 1996.

[8] J. Qian and A. Fatem, "Mixed Mode Fatigue Crack Growth: A Literature Survey," *Eng. Fract. Mech.*, **55**, 969–990, 1996.